chemistry proceedings

MDPI

Proceeding Paper

Theoretical Study of the Aza-Wittig Reaction, $Me_3P=NR$ (R = Methyl or Phenyl) with Aldehyde Using the DFT and DFT-D Methods (Dispersion Correction) †

Abdelghani Adda [1,2,*] and Hayat Sediki [1,3]

[1] LCPM, Chemistry Department, Faculty of Sciences, University of Oran 1, Ahmed Benbella, Es-Senia, Oran 31000, Algeria; sedikih@yahoo.fr
[2] Research Centre in Analytical Chemistry and Physics (CRAPC), BP 248, Algiers RP, Algiers 16004, Algeria
[3] Department of Materials Technology, Faculty of Physics, University of Science and Technology Mohamed Boudiaf, Oran 31000, Algeria
* Correspondence: adda20052000@yahoo.fr
† Presented at the 24th International Electronic Conference on Synthetic Organic Chemistry, 15 November–15 December 2020; Available online: https://ecsoc-24.sciforum.net/.

Abstract: The Aza-Wittig reaction plays an important role in organic transformations and has seen considerable development in the construction of cyclic and acyclic compounds in neutral solvents in the absence of catalysts with a high yield of products. Today, the use of iminophosphoranes (phosphazenes) has become a powerful tool in organic synthesis strategies directed toward the construction of nitrogenous heterocycles. These can react with carbonyl compounds, an excellent method for the construction of C=N double bonds via intermolecular and intramolecular Aza-Wittig reactions. In this study, we are interested in the theoretical study of the reaction path of the Aza-Wittig reaction between trimethyl-iminophosphoranes $(CH_3)_3P=NR$, R = CH_3 or Ph) for the two-substituent methyl and phenyl with acetaldehyde, including continuum solvation. Our calculations were carried out by means of ab initio calculations using DFT (Density Function Theory) with a dispersion correction term using the Grimme method in the program Gaussian09, using the functional B3LYP-GD3BJ with a 6-31G** base. The results obtained allowed us to highlight the mechanisms of the Aza-Wittig reaction in particular after the addition of the term of dispersion correction or van der Waals correction, which provides a new description of this reaction and its chemical path.

Keywords: Aza-Wittig; phosphazenes; trimethyl-iminophosphoranes; DFT; dispersion correction; van der Waals correction

Citation: Adda, A.; Sediki, H. Theoretical Study of the Aza-Wittig Reaction, $Me_3P=NR$ (R = Methyl or Phenyl) with Aldehyde by the DFT and DFT-D Methods (Dispersion Correction). *Chem. Proc.* **2021**, *3*, 47. https://doi.org/10.3390/ecsoc-24-08349

Academic Editors: Julio A. Seijas and M. Pilar Vázquez-Tato

Published: 14 November 2020

1. Introduction

Phosphazenes (iminophosphoranes) of the simple structure $R_3P=NR'$ were first described by Staudinger and Meyer in 1919 [1], but their applications only began in the 1950s. There are different names to designate this chemical function P=N, such as iminophosphorane, phosphinimine, λ-phosphazene, or phosphinimide.

However, compared to extensive studies of the Wittig reaction [2–17], little attention has been paid to the Aza-Wittig reaction. In 1997, Jugo Koketsu and colleagues [18] are the first to investigate the Aza-Wittig reaction of iminopnictoranes (H_3NMH, M = P, As, Sb, and Bi) with formaldehyde (H_2CO) at the MP2 level. They came to the conclusion that the Aza-Wittig reaction was more favorable for phosphorus for As, Sb, and Bi.

The Aza-Wittig reaction is arguably the most important reaction in the iminophosphorane reactivity panel. To elucidate the mechanism of Aza-Wittig reactions, it is important to isolate their intermediates, although such isolations are generally difficult due

to their instability. This reaction consists of a nucleophilic attack of the iminophosphoranes on the carbonyl (or thio-carbonyl) derivatives, followed by the removal of phosphine oxide (or phosphine sulfide). This reactivity very clearly resembles that of phosphorus ylides (Scheme 1), thus giving its name.

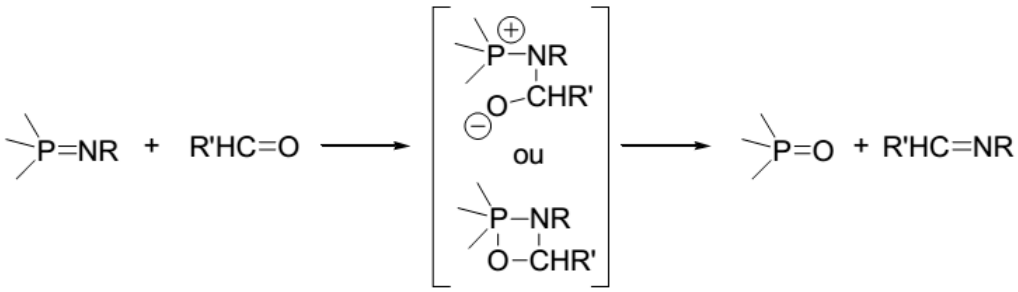

Scheme 1. Scheme showing two possible paths of the Aza-Wittig reaction mechanism.

The mechanism of the Aza-Wittig reaction is broadly known; we know in particular that it has two stages with fairly similar speeds. On the other hand, little experimental data are available on the intermediates (betaine or oxazaphosphetidine) of the reaction path, even if some special cases have been studied and characterized [12,13]

The greatest advances in the mechanism of the Aza-Wittig reaction have been made by theoretical studies of the reaction path using post Hartree–Fock methods such as Møller–Plesset at orders 2 and 4 and DFT [14–16]

As part of this work, we studied the reaction of Aza-Wittig for the two substituents of R, methyl and phenyl $(CH_3)_3$=NR with acetaldehyde (C_2H_4O) (see Figure 1). However, to our knowledge, no theoretical study on the DFT-D calculation (van der Waals dispersion correction) has been published on the Aza-Wittig reaction. The present work can provide theoretical information on this reaction.

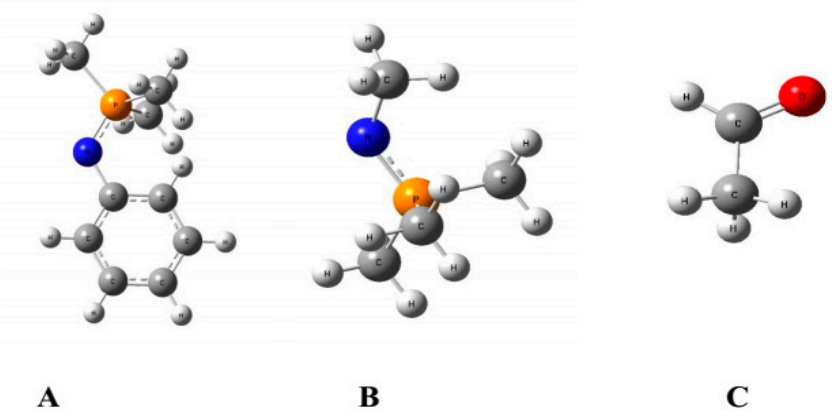

Figure 1. Optimized geometries of the reagents used in the Aza-Wittig reaction mechanism with (**A**)–(**C**) representing phosphazene with phenyl, phosphazene with methyl, and acetaldehyde, respectively.

2. Computational Methods

All the calculations reported in this paper were performed within density functional theory using the functional B3LYP [19,20] and B3LYP-GD3BJ (empirical dispersion) with a base 6-31G** [21]. Each point of the reaction path was fully optimized and verified to be a transition state (TSX) with imaginary frequency or stable species with real frequencies (i.e., RC "reagents", "intermediate" INX and PC "products"). Frequency analysis was performed to obtain thermochemical information about the reaction processes at 298 K. All

calculations are performed using the Gaussian-09 program, and the resulting surfaces were visualized using GaussView 6. IRC (intrinsic reaction coordinate) calculations were also performed to confirm the nature of the transition states.

Single-point energy calculations were also carried out for all species involved in the reaction at gas phase B3LYP-GD3BJ/6-31G** optimized geometries in THF (tetrahydrofuran) solvent using the integral equation formalism polarizable continuum model (IEFPCM).

3. Results and Discussion

3.1. Reaction of Methylimino(trimethyl)phosphorane with Acetaldehyde

Using DFT calculations at the B3LYP/6-31G** and B3LYP-GD3BJ/6-31G** level, it was shown that the reaction of the Aza-Wittig continues through $(CH_3)_3P = NCH_3 + O=CH2CH3 \rightarrow RC \rightarrow TS1 \rightarrow IN1 \rightarrow TSr \rightarrow IN2 \rightarrow TS2 \rightarrow PC \rightarrow (CH_3)_3P = O + CH_3N=CH_2CH_3$, where RC and PC represents a reactive and product complex, TS represents a transition state, and IN represents an intermediate state Scheme 2.

In our work, we found that the Aza-Wittig reaction between iminophosphorane and aldehyde is strongly exothermic and involves a stable [2 + 2] cycloaddition–cycloreversion sequence, with two intermediates IN1 and IN2 (Figure 2).

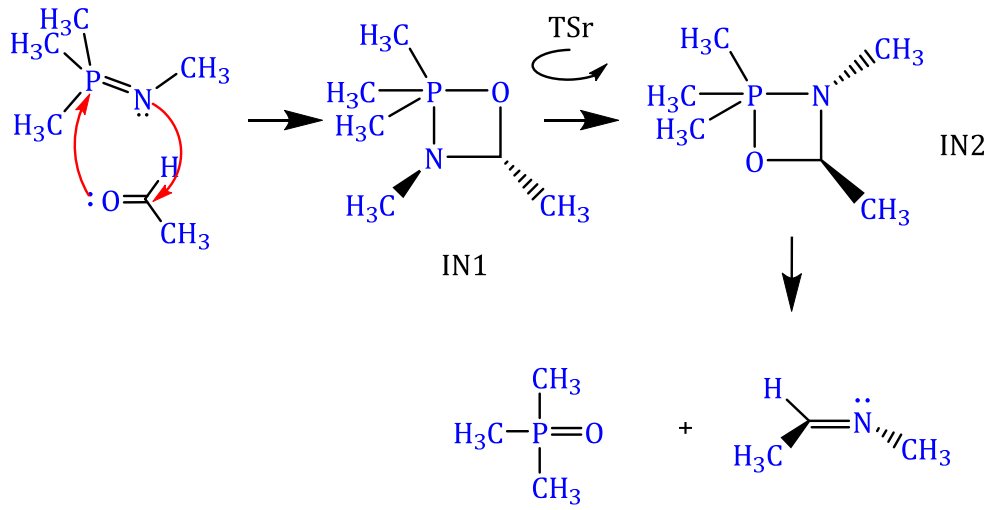

Scheme 2. Mechanism of Aza-Wittig reaction (methylimino(trimethyl)phosphorane with acetaldehyde).

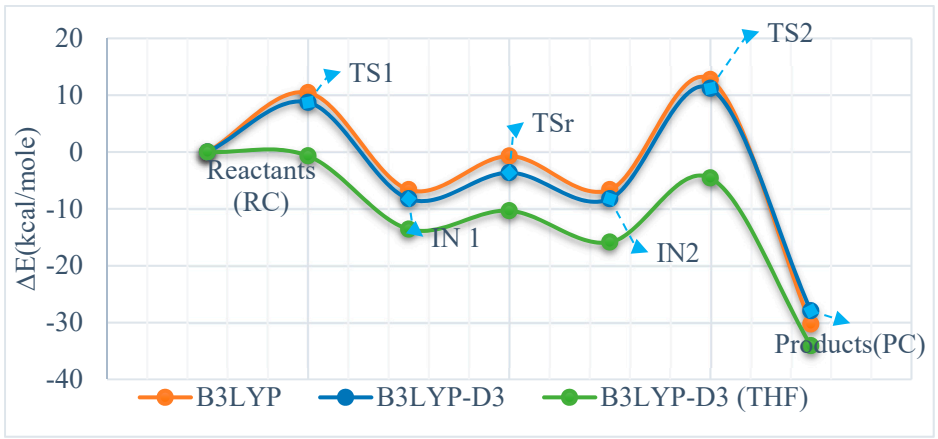

Figure 2. Potential energy diagram of the reaction of Aza-Wittig of methylimino(trimethyl)phosphorane with acetaldehyde in gas phase B3LYP, B3LYP-D3 and with solvent B3LYP-D3 (tetrahydrofuran (THF)).

The first TS1 transition structure was located at only 10.44 and 8.73 kcal/mol, for B3LYP and B3LYP-D3, above the reactants, which corresponds to a supra–supra geometry (see Table 1). This first cycloaddition [2 + 2] turns out to be quite asynchronous (Table 2), with a calculated synchronicity of 0.93 and 0.94. This observation is consistent with the analysis performed by McEwen for the similarity reaction of Wittig on the binding order using a semi-empirical method, which showed that the new C–C bond is formed at about 40% in the TS, while the P–O binding is still negligible at this stage [22,23]. The addition barrier is high in the B3LYP functional compared to the addition barrier in B3LYP-D3, after incorporation of dispersion corrections.

Table 1. Relative energies, enthalpy, and Gibbs free energy (kcal/mol) calculated using DFT, at B3LYP and B3LYP-D3 with a base of 6-31G** (D: dispersion corrections of Grimme).

Structures	(B3LYP)			(B3LYP-D3)		
	ΔE (kcal/mol)	ΔG (kcal/mol)	ΔH (kcal/mol)	ΔE (kcal/mol)	ΔG (kcal/mol)	ΔH (kcal/mol)
Reactants (RC)	0.00	000	0.00	0.00	0.00	0.00
TS1	10.44	14.77	10.28	8.73	12.17	8.52
IN 1	−6.63	−0.05	−5.01	−8.23	−2.46	−6.62
TSr	−0.71	6.44	−0.98	−3.63	2.75	−2.85
IN2	−6.63	−0.05	−5.01	−8.23	−2.46	−6.62
TS2	12.75	17.97	12.80	11.20	16.06	11.32
Products (PC)	−30.27	−29.31	−29.53	−27.94	−26.90	−27.15

Table 2. Bond lengths (in Å) and dihedral angles (in degrees) of the Aza-Wittig reaction of $Me_3P{=}NCH_3$. RC, reactive complex; TS, transition state; IN, intermediate; PC, product complext.

B3LYP/6-31G** B3LYP-D3/6-31G**	d_{P-N} Ångström	d_{C-O} Ångström	d_{P-O} Ångström	d_{N-C} Ångström	Φ_{PNCO}
Reactants (RC)	1.58	1.22	3.63	3.07	−2.42
	1.58	1.22	3.45	2.84	−0.50
TS1	1.64	1.28	2.69	1.76	−7.30
	1.63	1.28	2.70	1.76	−6.75
IN1	1.72	1.40	1.84	1.47	−6.73
	1.71	1.40	1.84	1.46	−6.95
TSr	1.81	1.42	1.73	1.45	−11.76
	1.81	1.43	1.73	1.45	−11.66
IN2	1.72	1.40	1.84	1.47	−6.75
	1.71	1.40	1.84	1.46	−6.95
TS2	2.42	1.69	1.59	1.36	8.58
	2.41	1.69	1.59	1.36	10.20
Products (PC)	4.13	3.76	1.51	1.27	−2.11
	3.89	3.53	1.51	1.27	−2.01

We also found an IN1 reaction intermediate of oxazaphosphetidine, in which the P=O bond was 1.84. Our results also indicated that IN2 is a fairly stable reaction intermediate.

In the intermediary of IN1, the coordination geometry around phosphorus was approximately a trigonal bipyramid, with oxygen derived from the aldehyde group found at the apical position. This then underwent pseudo-rotation on a low barrier to give an IN2 isomer with the iminophosphorane nitrogen in the apical position (IN2) (see Table 3).

Table 3. Optimized geometries of structures involved in the reaction pathway.

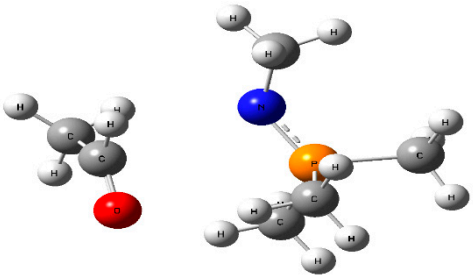	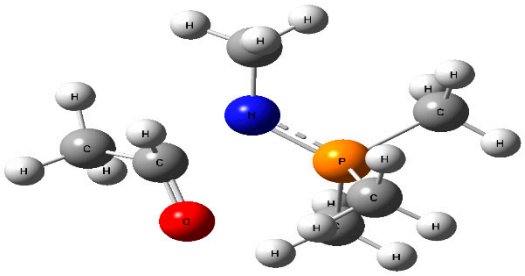
Reactants (RC)	TS1
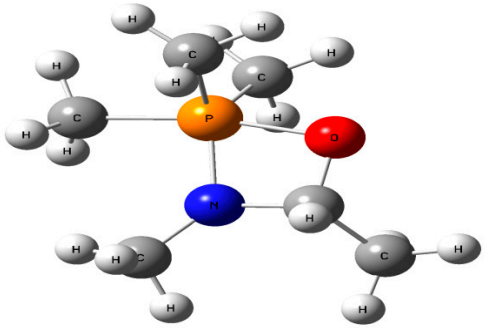	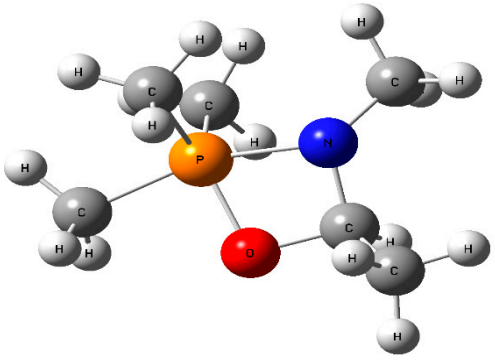
IN1	TSr
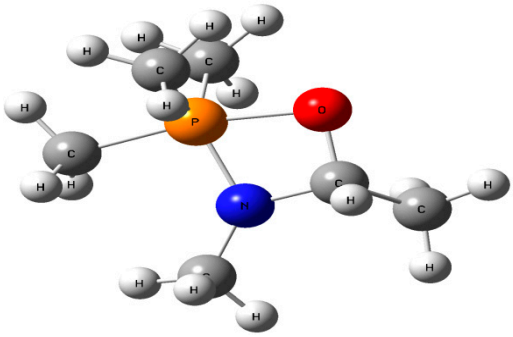	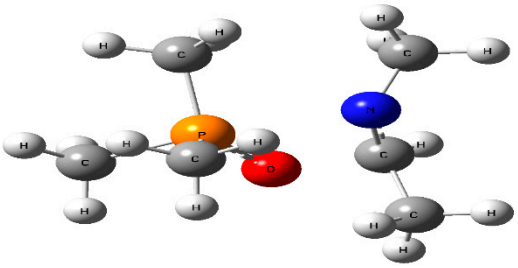
IN2	TS2
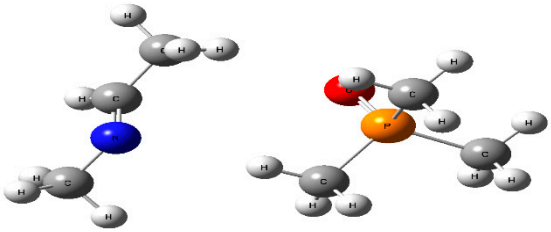	
Products (PC)	

The IRC calculations performed for the three TSs (TS1, TSr, TS2) showed that the localized TSs are well connected to the intermediates and final products. Indeed, optimizing the geometry of the last structure obtained on the IRC curve in the intermediate direction to IN1, IN2, and products gave a structure identical to the intermediate IN1, IN2, and final product.

The cycloreversion step [2 + 2] of the reaction took place from IN2 to TS2 had an activation energy greater than that calculated for the first step in Table 4; the incorporation of dispersion correction in functional B3LYP decreased the energy of activation corresponding to cycloaddition–cycloreversion of oxazaphosphetidine. With the effects on the molecular structure of the products being minor, this difference can be explained by the emergence of a dipole–dipole interaction between the two reagents at the addition. Note that the addition of the dispersion correction in the Hamiltonian more precisely in the exchange and correlation equation, for the functional B3LYP, slightly stabilized the structures of intermediates via cycloaddition. Thus, the addition process is more favored kinetically.

On the other hand, for the energy calculation including dispersion correction, B3LYP-D3/6-31G** (THF) seems to underestimate the energy barriers by −0.69 kcal/mol compared to that calculated at B3LYP-D3/6-31G**. The energy values for the addition steps with addition of solvent and dispersion correction were estimated to be −13.57 kcal/mol. Lower energy barriers suggest that the inclusion of dispersion correction and solvent had a significant effect on the reaction. For the second stages, the energy values were −15.86 kcal/mol.

Table 4. Activation energy corresponds to cycloaddition–cycloreversion of oxazaphosphetidine for B3LYP, B3LYP-D3.

	$\Delta G^{\neq}_{B3LYP}$	$\Delta G^{\neq}_{B3LYP-D}$
RC → TS1	14.77	12.17
IN2 → TS2	18.01	18.52

Table 5 shows that the negatively charged iminophosphorane nitrogen was attracted to the carbon atom of the positive charge aldehyde in TS1 because there was a wide region of negative electrostatic potential around the nitrogen atom, which confirmed the negative charge in the carbon; this charge decreased in the intermediate oxazaphosphetidine IN1. These potential electrostatic surfaces also support the initial stages of the reaction path in which a nucleophilic attack of nitrogen against the carbon aldehyde occurred.

Table 5. Maps of total electron density and calculated electrostatic potential for TS1 and intermediates IN1; regions of highest electron density distribution are displayed in intense red (−16.31 kcal/mol) and regions of density distribution lower electronics in intense blue (+16.31 kcal/mol).

TS1	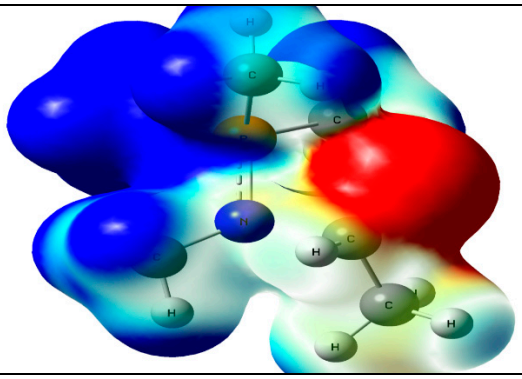

IN1 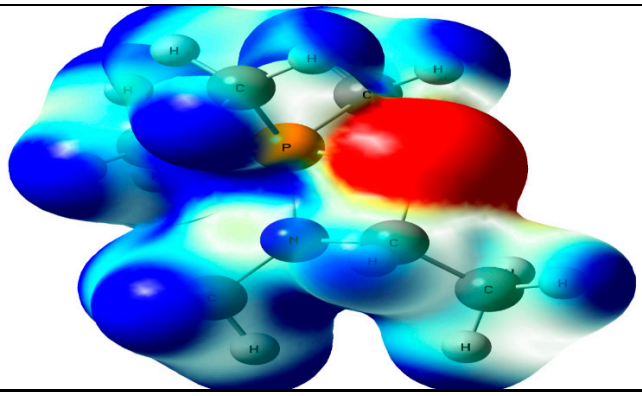

3.2. Reaction of Phenylimino(trimethyl)phosphorane with Acetaldehyde

Structure, geometric data and relative energies corresponding to the reaction of phenylimino(trimethyl)phosphorane ($(CH_3)_3P=NPh$) with acetaldehyde ($CH_3C=O$) at B3LYP and B3LYP-D3/6-31G** are given in Tables 6–8.

Table 6. Bond lengths (in Å) and dihedral angles (in degrees) of the Aza-Wittig reaction of methylimino(trimethyl)phosphorane with acetaldehyde $(CH_3)_3P=NPh$.

B3LYP/6-31G** B3LYP-D3/6-31G**	d_{P-N} Ångström	d_{C-O} Ångström	d_{P-O} Ångström	d_{N-C} Ångström	Φ_{PNCO}
Reactants (RC)	1.59	1.22	3.60	3.12	−3.38
	1.59	1.22	3.46	2.89	0.72
TS1	1.65	1.29	2.55	1.74	−7.29
	1.64	1.29	2.57	1.73	−8.33
IN 1	1.73	1.40	1.84	1.47	−5.42
	1.72	1.40	1.84	1.47	−5.35
TSr	1.93	1.45	1.68	1.44	−4.88
	1.91	1.45	1.68	1.43	−5.37
IN2	1.92	1.44	1.68	1.44	−3.55
	1.90	1.44	1.69	1.44	−3.71
TS2	2.60	1.62	1.59	1.38	1.77
	2.50	1.58	1.60	1.39	8.90
Products (PC)	4.05	3.21	1.51	1.28	9.05
	3.75	2.97	1.51	1.28	11.62

The first transition state TS had an almost planar structure TS1, in which the dihedral angle Φ_{PNCO} = −7.29 and −8.33 (for B3LYP-D3); for the second transition state, TS2 took the values of Φ_{PNCO} = 1.77 and 8.90. As shown in Figure 3, the second TS barrier was lower compared to TS1, which may explain kinetically why the reaction with phenyl as a substituent in the Aza-Wittig reaction was more stable and why the reaction took place rapidly in the second elimination step, i.e., cyclorevision of imine. Therefore, the Aza-Wittig reaction can be much more kinetically favorable for CH_3 in the first cycloaddition step and less favorable in the cycloreversion step, in contrast to the case where the phenyl substituent is bonded in imionphosphrane, with regard to the thermodynamic stability reaction with CH_3 which is more favored over phenyl.

Table 7. Optimized geometries of structures involved in the reaction pathway.

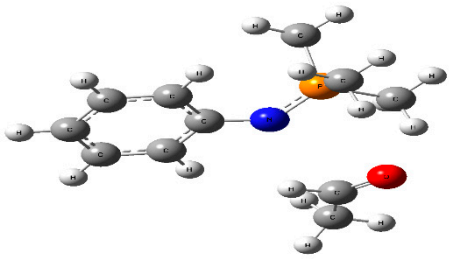	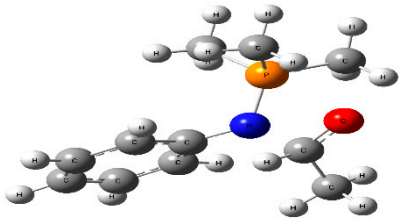
Reactants (RC)	TS1
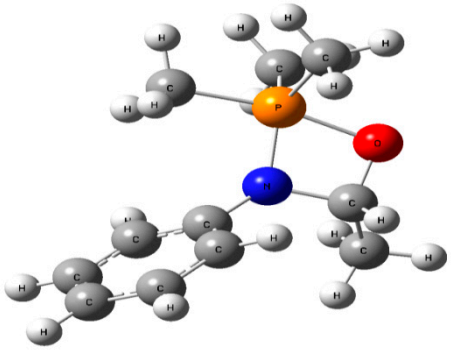	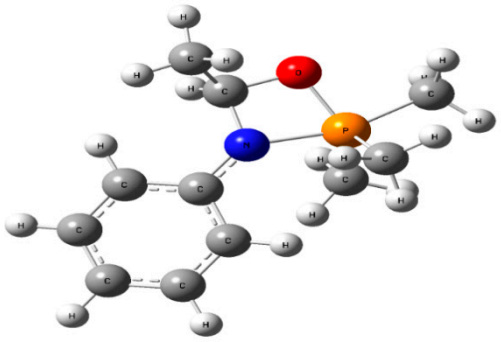
IN1	TSr
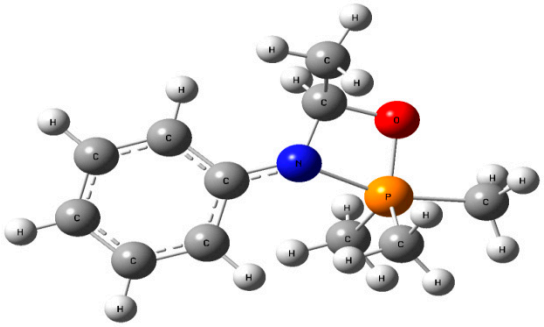	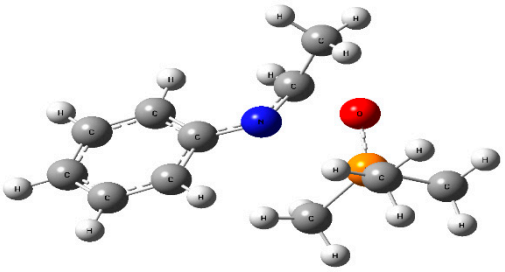
IN2	TS2
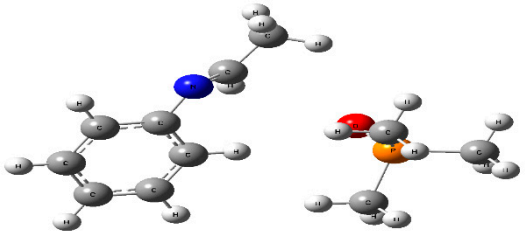	
Products (PC)	

The relative energies, enthalpy, and free energy for intermediates and transition states were more stable for functional B3LYP-D3 compared to B3LYP, without dispersion correction. Neglecting dispersion correction with solvent appeared to lead to a huge overestimation of the activation barriers by a single point at B3LYP-D3/6-31G** (THF). Thus, inclusion of dispersion correction significantly lowered the activation barriers for the reaction (see Figure 3).

Table 8. Relative energies, enthalpy, and Gibbs free energy (kcal/mol) calculated using DFT, at the theoretical level B3LYP and B3LYP-D3 with a base of 6-31G**.

Structures	(B3LYP)			(B3LYP-D3)		
	ΔE (kcal/mol)	ΔG (kcal/mol)	ΔH (kcal/mol)	ΔE (kcal/mol)	ΔG (kcal/mol)	ΔH (kcal/mol)
Reactants (RC)	0	0	0	0.00	0.00	0.00
TS1	15.88	19.05	15.59	13.76	16.30	13.40
IN 1	1.69	7.36	3.03	−0.11	3.69	1.15
TSr	2.18	9.21	3.00	0.23	6.08	0.99
IN2	0.66	7.51	2.15	−1.30	4.37	0.14
TS2	10.23	14.87	10.24	8.85	13.31	8.98
Products (PC)	−24.35	−23.29	−23.67	−22.55	−21.48	−21.89

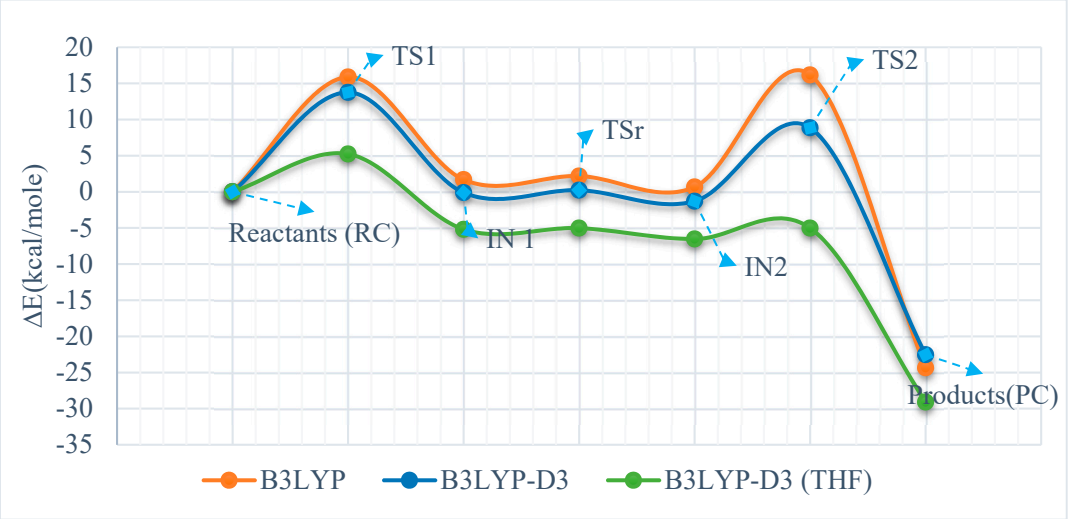

Figure-3. Potential energy diagram of the reaction of Aza-Wittig of phenylimino(trimethyl)phosphorane with acetaldehyde in gas phase B3LYP, B3LYP-D3 and with solvent B3LYP-D3 (THF).

The activation energies of addition and elimination are reported in Table 9. The addition TS1 have an energy high than the elimination TS2 (the direct barriers to the decomposition of the IN2 are less than the return barrier IN1). This means that the oxaphosphetane formation step must be irreversible.

Table 9. Activation energy corresponding to cycloaddition–cycloreversion of oxazaphosphetidine for functional B3LYP, B3LYP-D3.

	$\Delta G^{\neq}_{B3LYP}$	$\Delta G^{\neq}_{B3LYP-D}$
RC → TS1	19.05	16.30
IN2 → TS2	7.35	8.93

Table 10 shows that the negatively charged iminophosphorane nitrogen was attracted to the positive charge of the carbon atom of aldehyde in TS1, because there was a wide region of negative electrostatic potential around the nitrogen atom, which confirmed the negative charge in the carbon; this charge decreased in the intermediate oxazaphosphetidine IN1. These potential electrostatic surfaces also support the initial stages of the reaction path in which a nucleophile attack of nitrogen against the carbon aldehyde occurred.

Table 10. Maps of total electron density and calculated electrostatic potential for TS1 and intermediates IN1; regions of highest electron density distribution are displayed in intense red (−16.31 kcal/mol) and regions of density distribution lower electronics in intense blue (+16.31 kcal/mol).

TS1	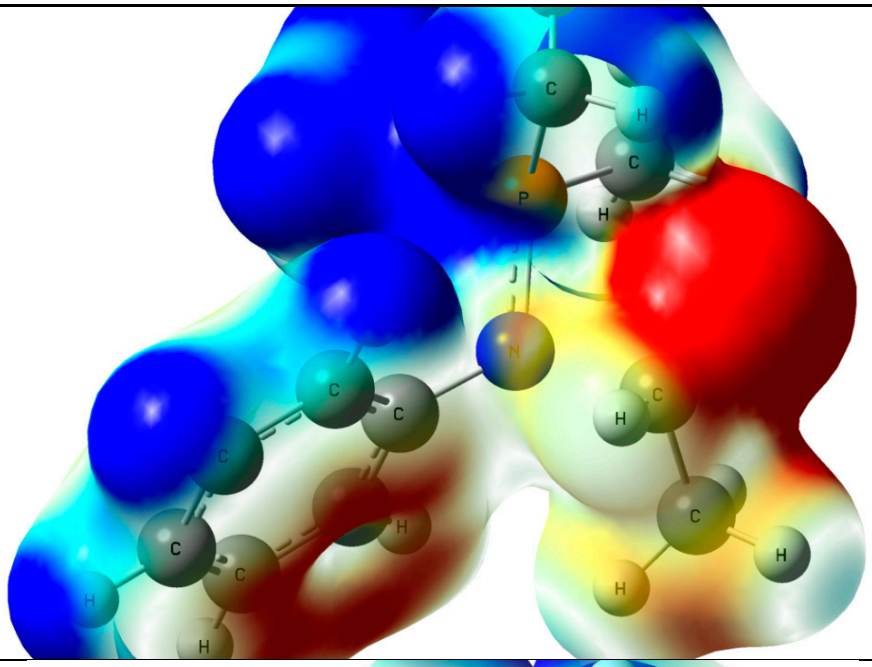
IN1	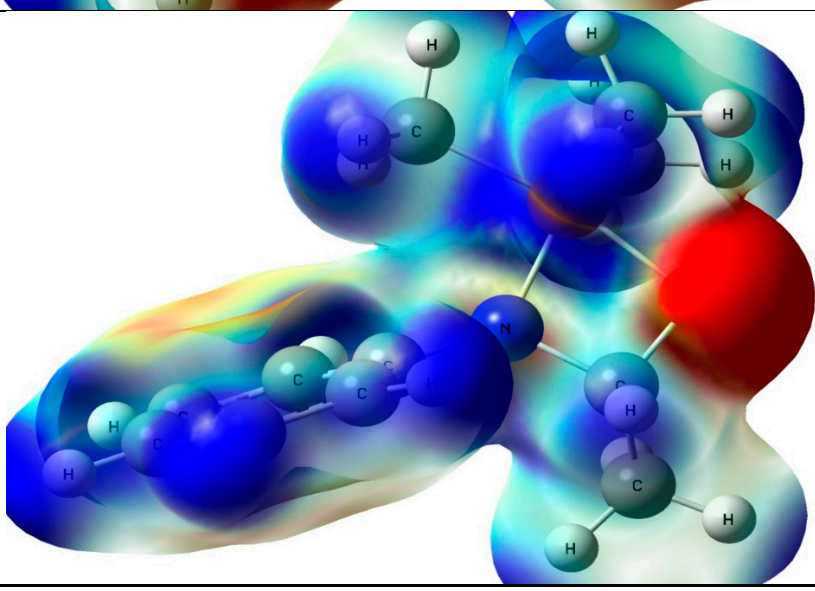

4. Conclusions

The Aza-Wittig reaction of trimethyliminophosphorane $(CH_3)_3P{=}NR$ for both methyl and phenyl substituents was investigated by means of ab initio calculations using DFT and DFT-D (dispersion correction) on the basis of 6-31G**. We conclude in this study that the Aza-Wittig reaction between phosphazenes and aldehydes takes place via a [2 + 2] cycloaddition–cycloreversion mechanism, with oxazaphosphetidines being the reaction intermediates. The two processes [2 + 2] are associated with thermally authorized asynchronous processes.

Methylimino(trimethyl)phosphorane is more reactive than phenylimino(trimethyl)phosphorane and less reactive in the second stage of elimination, i.e., cyclorevision of imine. Intermediate oxazaphosphetidines are four-membered rings in which the nitrogen atom is pyramidal. However, the energy barriers associated with the rotational movement are localized between the two intermediates; therefore, only the second stage leads

to the imines and phosphine oxides. The addition of the dispersion correction brings a new description of the reaction and the path of the chemical reaction, because it makes it possible to find a better description of the dispersion interactions in the description of the corrected functions using the DFT method.

Author Contributions: Calculation resources: A.A. and H.S. All authors have read and agreed to the published version of the manuscript.

Institutional Review Board Statement: Not applicable.

Informed Consent Statement: Not applicable.

Data Availability Statement: All data are available in the manuscript

Acknowledgments: The authors are deeply grateful to the University of Oran (Algeria) for computing resources and computer time used on Haytham at the UCI (Unité de Calcul Intensif), and to the University of Reims Champagne Ardennes (URCA, France) for computing resources and computer time used on Romeo calculator and Al-Farabi Cluster computer of the Ecole Nationale Polytechnique Oran—Maurice Audin.

References

1. Staudinger, H. New organic compounds of phosphorus. III. Phosphine-methylene derivatives and phosphinimines. *Helv. Chim. Acta* **1919**, *2*, 635–646.
2. Naito, T.; Nagase, S.; Yamataka, H. Theoretical study of the structure and reactivity of ylides of N, P, As, Sb, and Bi. *J. Am. Chem. Soc.* **1994**, *116*, 10080–10088.
3. Volatron, F.; Eisenstein, O. Wittig versus Corey-Chaykovsky Reaction. Theoretical study of the reactivity of phosphonium methylide and sulfonium methylide with formaldehyde. *J. Am. Chem. Soc.* **1987**, *109*, 1–14.
4. Streitwieser Jr, A.; Rajca, A.; McDowell, R.S.; Glaser, R. Semipolar phosphorus-oxygen and phosphorus-carbon bonds. A theoretical study of hypophosphite and related methylenephosphoranes. *J. Am. Chem. Soc.* **1987**, *109*, 4184–4188.
5. Dixon, D.A.; Smart, B.E. The structures and energetics of fluorine-substituted phosphonium ylides. *J. Am. Chem. Soc.* **1986**, *108*, 7172–7177.
6. Eades, R.A.; Gassman, P.G.; Dixon, D.A. The conformations and energetics of simple ylides. *J. Am. Chem. Soc.* **1981**, *103*, 1066–1068.
7. Vincent, M.A.; Schaefer III, H.F.; Schier, A.; Schmidbaur, H. Molecular and electronic structure of phosphonium cyclopropylide: a theoretical study. *J. Am. Chem. Soc.* **1983**, *105*, 3806–3811.
8. Hoeller, R.; Lischka, H. A theoretical investigation on the model Wittig reaction PH_3CH_2+ CH_2O. fwdarw. PH_3O+ C_2H_4. *J. Am. Chem. Soc.* **1980**. *102*, 4632–4635.
9. Maryanoff, B.E.; Reitz, A.B. The Wittig olefination reaction and modifications involving phosphoryl-stabilized carbanions. Stereochemistry, mechanism, and selected synthetic aspects. *Chem. Rev.* **1989**, *89*, 863–927.
10. Lischka, H. Electronic structure and proton affinity of methylenephosphorane by ab initio methods including electron correlation. *J. Am. Chem. Soc.* **1977**, *99*, 353–360.
11. Nguyen, M.T.; Hegarty, A.F. An Ab initio study of the diadic prototropic tautomerism H_3PX⇄ H_2PXH (X= O, NH, CH_2). *J. Chem. Soc., Perkin Trans.* **1987**, *2*, 47–54.
12. Bachrach, S.M. Molecular structure of phosphonium ylides. *J. Org. Chem.* **1992**, *57*, 4367–4373.
13. Sasaki, T.; Eguchi, S.; Okano, T. Novel synthesis and reactivity of 4-azahomoadamant-3-ene and 4-aza-4-homobrend-3-enes via intramolecular aza-Wittig reactions. *J. Am. Chem. Soc.* **1983**, *105*, 5912–5913.
14. Sheldrick, W.S.; Schomburg, D.; Schmidpeter, A.;von Criegern, T. Four-And Five-Membered Phosphorus Heterocycles. 39. Structural Changes in The (2+ 2) Cycloaddition of Ketones to Azaphospholes. *Chem. Inf.* **1980**, *11*, 304.
15. Molina, P.; Alajarin, M.; Lopez Leonardo, C.; Claramunt, R.M.; Foces-Foces, M.D.L.C.; Hernandez Cano, F.; Catalan, J.; De Paz, J.L.G.; Elguero, J. Experimental and theoretical study of the R3P+-X-bond. Case of betaines derived from N-iminophosphoranes and alkyl isocyanates. *J. Am. Chem. Soc.* **1989**, *111*, 355–363.
16. Lu, W.C.; Liu, C.B.; Sun, C.C. Theoretical study of the H_3PNH+ H_2CO reaction mechanism via five reaction channels. J. Phys. Chem. A **1999**, *103*, 1078–1083.
17. Lu, W.C.; Sun, C.C.; Zang, Q.J.; Liu, C.B. Theoretical study of the aza-Wittig reaction X_3P = NH + O = CHCOOH → X_3P = O+ HN= CHCOOH for X = Cl, H and CH_3. *Chem. Phys. Lett.* **1999**, *311*, 491–498.
18. Koketsu, J.; Ninomiya, Y.; Suzuki, Y.; Koga, N. Theoretical study on the structures of iminopnictoranes and their reactions with formaldehyde. *Inorganic Chemistry* **1997**, *36*, 694–702.
19. Becke, A.D. Density-functional exchange-energy approximation with correct asymptotic behavior. *Phys. Rev. A* **1988**, *38*, 3098.
20. Lee, C.; Yang, W.; Parr, R.G. Development of the Colle-Salvetti correlation-energy formula into a functional of the electron density. *Phys. Rev. B* **1988**, *37*, 785.

21. Hariharan, P.C.; Pople, J.A. The influence of polarization functions on molecular orbital hydrogenation energies. *Theor. Chim. Acta* **1973**, *28*, 213–222.
22. Marí, F.; Lahti, P.M.; McEwen, W.E. Molecular modeling of the Wittig olefination reaction: Part 2: A molecular orbital approach at the MNDO-PM3 level. *Heteroat. Chem.* **1991**, *2*, 265–276.
23. Mari, F.; Lahti, P.M.; McEwen, W.E. Molecular modeling of the Wittig reaction. 3. A theoretical study of the Wittig olefination reaction: MNDO-PM3 treatment of the Wittig half-reaction of unstabilized ylides with aldehydes. *J. Am. Chem. Soc.* **1992**, *114*, 813–821.